agronomy

MDPI

Article

Vibration Response of Walnuts under Vibration Harvesting

Changyi Liu, Daochun Xu * and Jiale Cao

School of Technology, Beijing Forestry University, Beijing 100083, China
* Correspondence: xudaochun@bjfu.edu.cn; Tel.: +86-10-62338153

Abstract: Vibration harvesting is a promising method for walnut production owing to its low cost and high efficiency. However, current research focuses on simulation analysis and lacks a theoretical model explaining the walnuts' specific vibration response. This affects the design of the input vibration parameters during harvesting and thus reduces the harvesting efficiency. In this paper, a novel theoretical model of walnuts during vibration harvesting was established to analyze the vibration response, including the motion morphology (motion trajectory and dropping position) and detachment force. A field test was then carried out to verify the theoretical model. The theoretical and experimental results showed that the motion trajectory of the walnuts during vibration harvesting is similar to an ellipse, and the dropping position is at either of the two end points of the trajectory. The detachment force was found to be proportional to the vibration amplitude and the square of the vibration frequency theoretically. This paper provides a theoretical reference for designing the optimal input vibration parameters of a harvesting device to improve the harvesting rate of walnuts.

Keywords: walnut; fruit harvesting; vibration response; detachment force; fruit motion

check for updates

Citation: Liu, C.; Xu, D.; Cao, J. Vibration Response of Walnuts under Vibration Harvesting. *Agronomy* **2023**, *13*, 461. https://doi.org/10.3390/agronomy13020461

Received: 23 December 2022
Revised: 25 January 2023
Accepted: 1 February 2023
Published: 3 February 2023

Copyright: © 2023 by the authors. Licensee MDPI, Basel, Switzerland. This article is an open access article distributed under the terms and conditions of the Creative Commons Attribution (CC BY) license (https://creativecommons.org/licenses/by/4.0/).

1. Introduction

Forest fruits are produced in more than 170 countries, and their production contributes to the agricultural economy and farmers' income [1]. Fruit harvesting, an essential component in fruit production, is characterized by strong seasonality and high labor intensity [2]. The common method of harvesting forest fruits is the use of manual labor [3,4], but the cost of such harvesting is high, as the manual labor force accounts for a large proportion of the total labor force in the overall production process [2,5]. Mechanized harvesting is thus a crucial component in forest fruit production [6]. There are two categories of existing mechanized harvesting, namely individual harvesting and non-selective large-scale harvesting. The latter is especially suited to forest fruit species that have many small fruits per plant, except for some special cases, such as the need to harvest some fruits of certain maturity when there are fruits of different maturity on the same tree. Vibration harvesting, which applies a vibration force to trees to induce a detachment force on fruits [7], is a method commonly used in non-selective large-scale harvesting. Erdogan et al. found that vibrating mechanized picking is more than three times as efficient as manual and traditional picking [8]. Additionally, this method is ideal for fruits that have hard and impact-resistant shells, such as walnuts, as there is no damage to the fruits during vibration and detachment. Researchers have thus shown an increasing interest in the vibration harvesting of walnuts. Zhang et al. compared the binding force and pull-off force of the walnut fruit stalk, and proposed that picking walnuts through vibration is feasible, with the efficiency being two to three times that of manual picking [9].

In the vibration harvesting of walnuts, distinct vibration parameters generate different vibration responses in trees and fruits [7,10]. Many studies on the vibration response and vibration parameters of trees have focused on simulation models [7,8]. For example, scholars have carried out finite element simulations for olive [11], coffee fruit [12], and jujube [13]. These scholars discovered an intense vibration of fruit when the excitation frequency is close to the natural frequency of the fruit. This phenomenon, called resonance

harvesting, is considered to provide the best circumstances for the vibration harvesting of fruit. However, resonance collection on a large-scale is challenging under actual harvesting conditions owing to the limitations of simulation. For example, computer simulations only analyze the model of a single structure under ideal conditions, ignoring external factors such as the absorption of vibration energy by the soil, the aerodynamic damping of trees [14], and the differences between the structures of trees during field harvesting under actual conditions. The structures of trees vary and are intimately associated with the dynamic responses of the trees, and the diameter, crotch angle, and connection points of branches thus affect vibration transmission [7,8,10]. Although horticultural technology has been adopted to cultivate tree species with relatively regular shapes, such as the Y trellised Chelan species, whose branches are fixed at a 55-degree angle to the trunk [15], the natural frequencies of various maturation stages are notably different for the same tree [12]. Hence, it is difficult to realize resonance harvesting in a vast area of fruits using a single fixed frequency; instead, in the harvesting process, the frequency must be adjusted according to the specific conditions and the differences among the trees. Although He et al. devised a method for identifying the natural frequency of fruit trees on site, this method is limited to small and medium-sized fruit trees [16]. Moreover, as the natural frequencies of different branches vary, it is necessary to detect the natural frequency of each larger branch in achieving a high harvesting efficiency, and this method is thus time-consuming and inefficient in practical applications. Consequently, vibration harvesting at a single frequency cannot resonate each position on the tree as the different positions have a unique natural frequency based on their characteristics [17]. Furthermore, because the response frequency is attenuated relative to the input frequency [18], the maximum difference between the fruits' input frequency and response frequency can exceed 53% [19]. Accordingly, resonance harvesting is difficult to conduct by simply adjusting the input vibration frequency of the collection device to match the fruit's response frequency with its natural frequency. Therefore, it is imperative to study vibration harvesting under non-resonant conditions in improving the harvest rate. To research the non-resonant harvesting of walnuts, the relationship between the vibration response of fruits and various vibration parameters should be explored. Vibration parameters, especially the vibration frequency and amplitude, affect the vibration response of a single vibration [15,20–23], and several attempts have been made to study how these parameters affect the detachment force, response acceleration, or harvest rate, which can reflect the vibration response. Leone et al. showed that improving the detachment force requires a higher frequency and acceleration [19]. Andre et al. developed parameters for the coffee harvesting machine and discovered that the harvest rate increased over the same duration with increases in the vibration frequency and amplitude [24]. Savary et al. measured the response acceleration under different vibration parameters using simulation and experimental methods, showing that the response acceleration increased with the vibration frequency [25].

The existing research revealed that the vibration response is closely related to the vibration frequency and amplitude, and the degree of the vibration response increases with the vibration frequency and amplitude. However, the research to date has tended to focus on the harvesting results rather than the specific motion and dropping morphology of the walnut fruits in the actual vibration process. Without investigating the detachment mechanism of the walnut fruits under a vibration response, the exact equation relationship between the vibration response of fruits and the vibration frequency and amplitude cannot be established, leaving no theoretical guidance for practical application. Simultaneously, ignorance of a proper and effective combination of the frequency and amplitude in harvesting during the design and application of the vibration harvesting device [24,26] inevitably harms the trees and complicates the mechanical manufacturing through the selection of an excessive frequency or amplitude [27]. Hence, in this paper, a theoretical model exploring the motion and dropping morphology of the vibration response of walnuts under vibration harvesting is established and verified by conducting a field test. The functional relationship between the detachment force and the external vibration frequency and amplitude is fur-

ther obtained, which gives the relationship between the vibration response and vibration parameters. This paper reports on an in-depth study of the vibration response of walnuts, including the motion morphology and detachment force, and provides theoretical guidance for designing the optimal input parameters of a vibration harvesting device to improve the harvest rate of walnuts.

2. Theoretical Model of the Vibration Response of Walnuts

2.1. Force Analysis

In the actual measurement of fruit response acceleration, the method is usually to use sensors to measure the acceleration of fruit vibration response in x, y, and z directions and then sum their vectors to obtain the synthesized response acceleration of fruit to explore the vibration response. Therefore, in this paper, the method of synthesis and decomposition of motion and forces was used to establish a theoretical model to study the vibration response of walnuts. The response acceleration of the external vibration force transmitted from the tree trunk to the walnut fruits is the combination of horizontal and vertical accelerations, regardless of the type of vibration [13]. Figure 1 is a diagram of forces acting on the tree trunk and walnut fruit. F_0 is the vibration force applied to the tree trunk, θ_0 is the angle of the force F_0 relative to the horizontal direction, and F_1 is the excitation force transmitted to the walnut fruits. The excitation force F_1 is in the same direction as the vibrating force F_0 and can be divided into the vertical force F_{1V} and horizontal force F_{1H}. S_1 is the response amplitude, which can be resolved into the vertical amplitude S_{1V} and horizontal amplitude S_{1H}. Figure 2a shows the synthesized motion generated by horizontal and vertical forces. The synthesized motion and the vibration response of the walnut fruits can thus be determined by studying the motion generated by the excitation force in the horizontal and vertical directions, analyzing the position of the maximum force along with the actual force magnitude of synthesized motion, and synthesizing the motion and force in the two directions. The actual motion of the walnuts is reciprocating and symmetrical, and thus only half a cycle is discussed. Furthermore, the gravitational force acting on the fruit is neglected because it is much less than F_1.

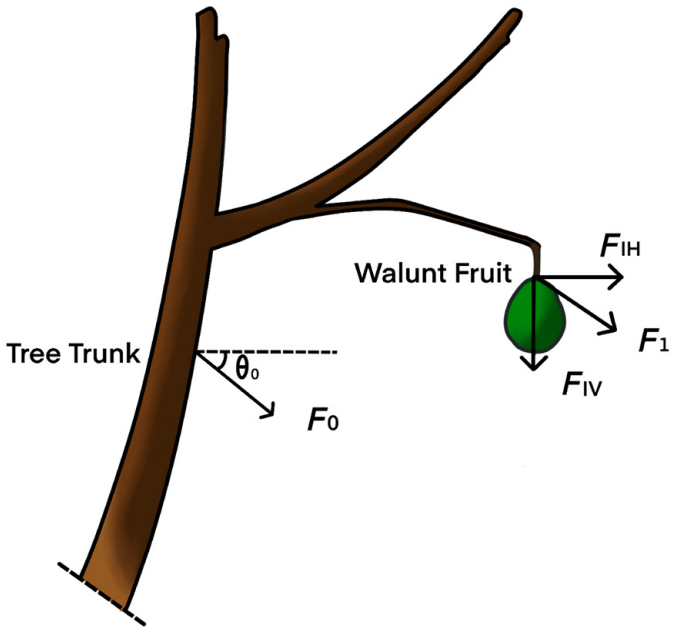


Figure 1. Forces acting on the tree branch and walnut fruit.

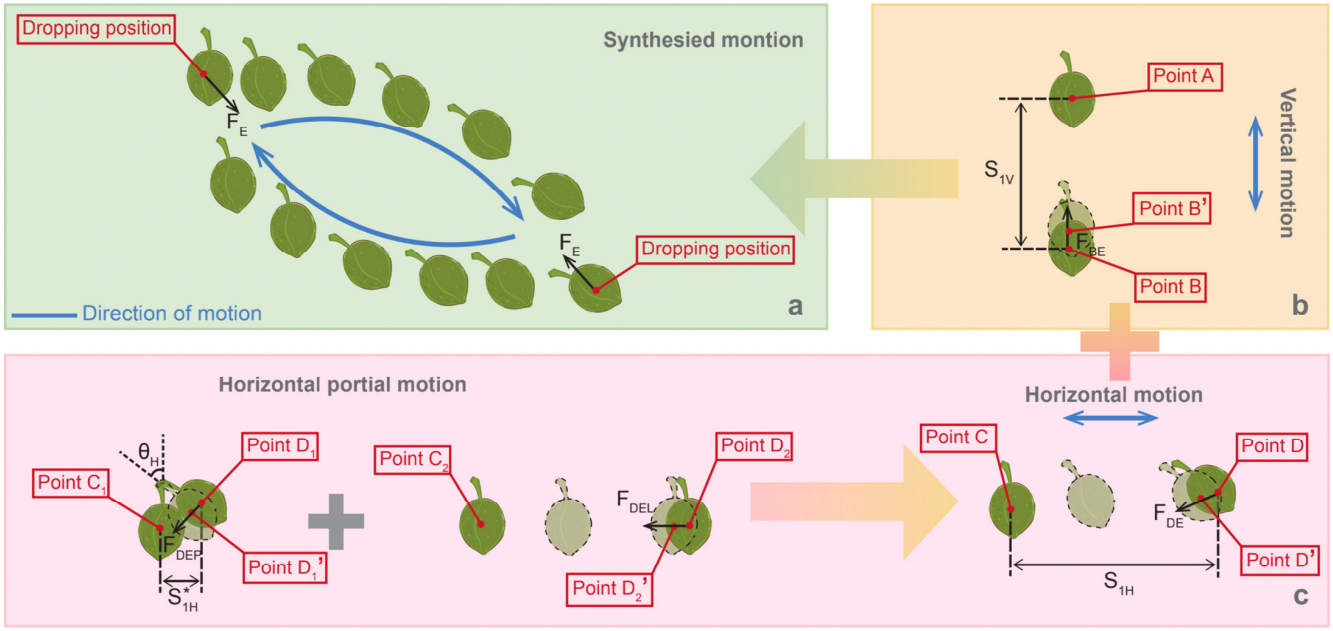


Figure 2. Schematic of the vibration response of walnuts: (**a**) synthesized motion; (**b**) vertical motion; (**c**) horizontal motion.

2.2. Vibration Response in the Vertical Direction

General analysis reveals that during the motion of walnut fruits from end point A to point B′ at which the velocity is maximum, the direction of the resultant external force F_{VE} is vertical and downward, with its magnitude constantly changing. This further indicates that the motion of walnuts is linear with varying and positive acceleration in the vertical direction. The velocity of the walnut fruits drops rapidly to zero as the fruits move from point B′ to the end point B, resulting in the walnut stalk exerting a tension force on the walnut fruits. As the stress of vibration in the vertical direction is a maximum at both ends and certain points under special circumstances [13], we chose a short period of time t, during which the acceleration a can be regarded as a quantitative, and the motion can be regarded as uniformly accelerated rectilinear motion. The acceleration a during this period is calculated as

$$a = \frac{\mathrm{d}v^2}{2\mathrm{d}x} \tag{1}$$

Equation (1) shows that the acceleration a reaches a maximum when v^2 changes the most over the shortest distance, and the force acting on the fruits is thus maximum. The fact that the velocity of the fruits at the two ends rapidly decreases to zero and that this velocity is the accumulation of acceleration over time throughout the cycle, while being the highest velocity in the process, implies that the acceleration is generally maximum at the end point in actual harvesting. Figure 2b shows that the resultant external force acting on the walnut fruits in the vertical direction is maximum at end point B and is set as the maximum detachment force F_{BE}. F_{VE} is the resultant external force when the walnut fruits move from end point A to end point B. As the vibration frequency is f_1, the half cycle duration is $1/2f_1$, which is the time required to move from end point A to point B′ in the vertical direction. This is because motion from point B′ to end point B, with the velocity of walnut fruits falling from a maximum to zero, takes little time. Theorems of kinetic energy and momentum are applied to the process from end point A to point B′.

$$\int_0^{S_{1V}} F_{VE} ds = \Delta E_K = \tfrac{1}{2} m v_{B'}^2, \tag{2}$$

$$\int_0^{\frac{1}{2f_1}} F_{VE}dt = \Delta p = mv_{B'} \tag{3}$$

where S_{1V} is the vertical component of the response amplitude, ΔE_K is the variation in kinetic energy, Δp is the variation in momentum, m is the weight of the walnut fruit, ds is the infinitesimal of distance during the kinetic energy change, and dt is the infinitesimal of time during the momentum change. Combining the above equations, the maximum velocity for walnut fruits at point B′ is calculated as $v_{B'} = 4\ S_{1V}f_1$. Here, t_{B0} is the time period during which the velocity around end point B decreases from $v_{B'}$ to zero. The momentum theorem is applied for this process:

$$\int_0^{\alpha_1 \frac{1}{2f_1}} F_{BE}dt = mv_{B'} \tag{4}$$

where we let the ratio of t_{B0} to the time period of half a motion cycle $1/2f_1$ be α_1, and the maximum detachment force in the vertical direction can be obtained as

$$F_{BE} = \frac{8m\sin\theta_0}{\alpha_1} S_1 f_1^2 = \vec{\varepsilon_1} S_1 f_1^2\ . \tag{5}$$

where m is the weight of walnut fruits, $sin\theta_0$ and α_1 are constants independent of the vibration parameters, and $\varepsilon_1 = 8msin\theta_0/\alpha_1$ is a vector of the direction with the maximum detachment force in the vertical direction.

2.3. Vibration Response in the Horizontal Direction

General analysis shows that during the motion of walnut fruits from point C to point D′ in the horizontal direction, the direction of the excitation force F_{1H} in forced vibration is horizontal and constantly changing. Moreover, the tension force exerted on walnut fruits by their fruit stalks acts as a centripetal force F_n aligned with the fruit stalk. Figure 2c shows that the motion of walnut fruits in the horizontal direction can be viewed as a pendulum motion along the fruit stalk of walnuts and linear motion with varied acceleration, with the maximum stress points of vibration in the horizontal direction appearing at both ends [13]. Therefore, the maximum force of the synthesized motion of walnut fruits in the horizontal direction can be obtained by analyzing the force at the end points of the pendulum motion and the linear motion with variable acceleration.

Similar to the analysis in the vertical direction, the time of motion of the walnut fruits from point C to point D′ is $1/2f_1$, and t_{D0} is the time period during which the velocity around end point D decreases from a maximum to zero. The ratio of t_{D0} to the time period of half a motion cycle, $1/2f_1$, is denoted as α_2, and the ratio of the distance of movement of the walnut pendulum in the horizontal direction, S_{1H}^*, to the total distance in the horizontal direction, S_{1H}, is denoted as γ_1. By referencing Equations (2) and (3) in Section 2.2, the maximum velocity of walnut fruits from point C_2 to point D_2 for linear motion with varying acceleration is obtained as $v_{D'L} = 4S_{1H}f_1$. Using Equation (4), the maximum force at the end point D'_2 is calculated as

$$F_{DEL} = \frac{8m\cos\theta_0(1-\gamma_1)}{\alpha_2} S_1 f_1^2\ = \vec{\varepsilon_2} S_1 f_1^2 \tag{6}$$

With reference to the simplified analysis in Section 2.2, the constant $8\ mcos\theta_0(1\text{-}\gamma_1)/\alpha_2$ is expressed as ε_2, and the vector ε_2 is aligned with F_{DEL}.

Analysis of the horizontal pendulum of walnut fruits reveals that throughout the motion from point C_1 to point D_1, the horizontal component of the excitation force F_{1H} is the only factor that affects the kinetic energy. In contrast, the change in momentum is due to the resultant external force in the horizontal direction, F_{HE}, which comprises F_{1H} and the centripetal force F_n during pendulum. Theorems of kinetic energy and momentum are applied for this process.

$$\int_0^{S_{1H}^*} F_{1H}ds = \Delta E_K = \frac{1}{2}mv_{D'P}^2 \tag{7}$$

$$\int_0^{\frac{1}{2f_1}} F_{HE}dt = \Delta p = mv_{D'P} \tag{8}$$

$$v_{D'P} = \sqrt{v_{D'Px}^2 + v_{D'Py}^2} \tag{9}$$

The maximum velocity when the pendulum reaches point D'$_1$, $v_{D'P}$, is decomposed into the horizontal velocity $v_{D'Px}$ and the vertical velocity $v_{D'Py}$.

The vertical and horizontal momentum theorems are then applied for the pendulum process.

$$mv_{D'Px} = \int_0^{\frac{1}{2f_1}} (F_{1H} - F_n \sin\theta_H)dt, \tag{10}$$

$$mv_{D'Py} = \int_0^{\frac{1}{2f_1}} F_n \cos\theta_H dt \tag{11}$$

where θ_H is the maximum pendulum angle in the horizontal direction, and the kinetic energy theorem is applied for any moment during pendulum.

$$\int_0^{S_i} F_{1H}ds = \Delta E_K = \frac{1}{2}mv_i^2 \tag{12}$$

where v_i is the velocity at that particular moment. By combining the centripetal force equation $F_n = mv_i^2/R$ with Equation (10), F_n is expressed as

$$F_n = \frac{2\int_0^{S_i} F_{1H}ds}{R} = \frac{2S}{R}F_{1H} = \beta_4 F_{1H}, \tag{13}$$

where S_i is the distance of the pendulum, and R is the length of the fruit stalk of a walnut. As both constants are independent of F_{1H}, β_4 is used in place of $2S_i/R$. By combining Equations (7)–(11) and (13), the maximum velocity when the pendulum in the horizontal direction reaches point D is expressed as

$$v_{D'P} = \frac{4S_{1H}^* f_1}{\sqrt{1 + \beta_4^2 - 2\beta_4 \sin\theta_H}} \tag{14}$$

As a partial motion of the horizontal synthesized motion, the ratio of the time when the velocity around end point D_1 decreases from $v_{D'P}$ to zero to the time for a half cycle is α_2, the same as the condition at end point D_2. The momentum theorem is applied for this process.

$$\int_0^{\alpha_2 \frac{1}{2f_1}} F_{DEP}dt = mv_{D'P} \tag{15}$$

The maximum force of the pendulum is obtained as

$$F_{DEP} = \frac{8m\cos\theta_0\gamma_1}{\alpha_2\sqrt{1 + \beta_4^2 - 2\beta_4 \sin\theta_H}} S_1 f_1^2 = \vec{\varepsilon_3} S_1 f_1^2. \tag{16}$$

By referencing the simplified principle above, the constants can be expressed as ε_3, which is a vector aligned with F_{DEP}.

The analysis reveals that the force of the pendulum motion and linear motion with varying acceleration of walnuts is a maximum at point D in the horizontal motion. Therefore, the maximum resultant external force acting on the walnut fruits in the horizontal direction, namely the detachment force, is

$$F_{DE} = F_{DEL} + F_{DEP} = \left(\vec{\varepsilon_2} + \vec{\varepsilon_3}\right) S_1 f_1^2. \tag{17}$$

2.4. Synthesized Motion of the Vibration Response

The above analyses reveal that in half a cycle, the motion of the walnut fruits in the vertical direction is linear with variable acceleration, and the force is a maximum around end point B. The motion in the horizontal direction is pendulum and linear with variable acceleration, and the stress is a maximum around end point D. The synthesis of vertical and horizontal movements yields the synthesized motion of the walnuts. The walnuts move symmetrically in a cycle, and the total synthesized motion of walnut fruits can thus be obtained using the symmetry of motion in a half cycle. Accordingly, the actual situation of the total synthesized motion is shown in Figure 2a. As walnut fruits move to points B and D simultaneously, the stress of the total synthesized motion of walnuts is a maximum at the end point of the synthesized motion (i.e., the falling position illustrated in Figure 2), and the maximum detachment force is obtained as

$$F_E = F_{BE} + F_{DE} = (\vec{\varepsilon_1} + \vec{\varepsilon_2} + \vec{\varepsilon_3})\, S_1 f_1^2. \tag{18}$$

On account of a greater acceleration corresponding to a greater detachment force and thus a higher harvest rate [28], the detachment force reflects the vibration response. As a result, the theoretical Equation (18), which expresses the detachment force as being proportional to the vibration amplitude and the square of the vibration frequency, reflects the relationship between the vibration response and the response frequency and amplitude. Therefore, this equation shows from the relationship level that to obtain a high harvesting rate, the vibration parameters of frequency and amplitude should be comprehensively considered. Only when vibration frequency and amplitude both reach the appropriate combination, will the fruit vibration response be the best.

From the above theoretical analysis of the synthesized motion and decomposition motion in the vertical and horizontal direction, the motion trajectory can be regarded as a combined linear motion with variable acceleration in both horizontal and vertical directions because the displacement of the simple pendulum motion is small. As a result, the motion trajectory for a half cycle of the synthesized motion is an analogous parabola. As the synthesized motion is reciprocating and symmetrical, the motion trajectory of a walnut in one cycle resembles an ellipse. Additionally, the detachment mechanism of walnuts is derived through the above analysis of motion and Equations (4) and (15), and the direction of motion changes in a short period when the walnuts move to the two end points, which involves a rapid change in momentum. Therefore, a maximum detachment force is exerted on the walnuts, leading to the fall of the walnuts. The dropping positions of the walnuts are thus concentrated at the two end points of the motion trajectory, where the maximum force occurs.

3. Experimental Setup

The experiment reported in this paper was conducted in a walnut garden located in the northwest of Beijing, China, in September 2022. Eight of the twenty walnut trees in the garden were randomly chosen as the experimental samples. As shown in Figure 3, the experiment adopted a vibration harvesting device with adjustable frequency and amplitude. The device was powered by a motor (3 kW alternating-current motor, Zhejiang ANG Company, Hangzhou, China) controlled by a frequency converter (HK300, HORKE Company, Weihai, China). The rocker arm of the device was connected to the branch of the tree by a steel wire rope that transmitted the vibration. The vibration amplitude of the vibration harvesting device was controlled by altering the connecting position of the steel wire rope and the device's rocker arm, whereas the vibration frequency was adjusted by changing the input voltage frequency of the motor through the frequency converter. It was thus possible to investigate the vibration response of walnuts under different frequencies and amplitudes.

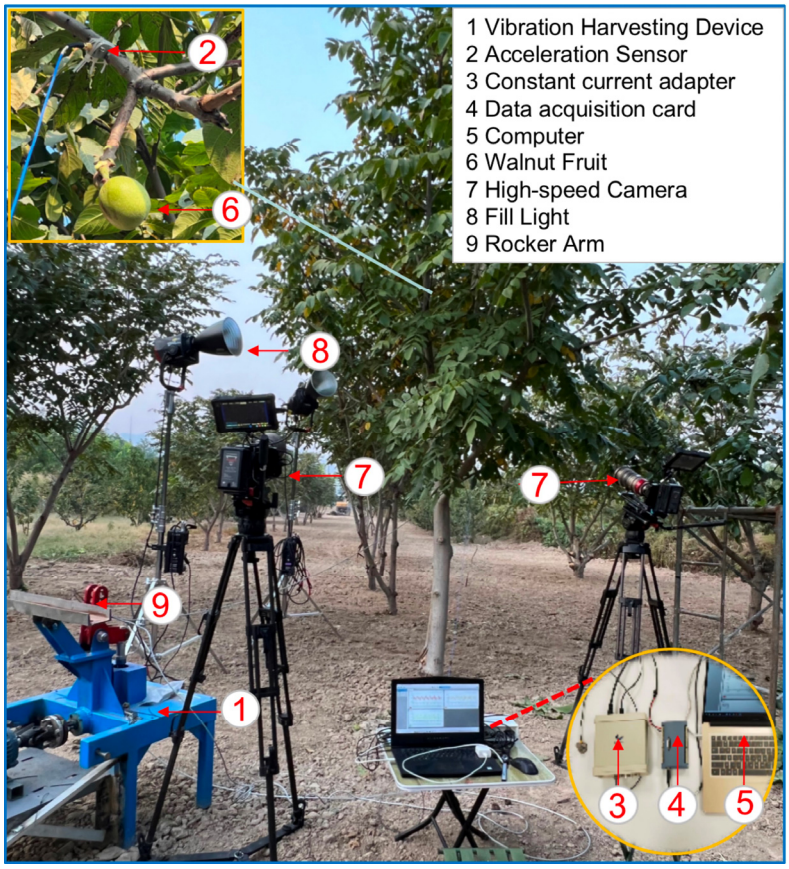


Figure 3. Setup of the field test.

The experimental dates were recorded by a triaxial acceleration sensor (1010LSPFP, Shanghai Chengtec Company, Shanghai, China). The sensor was fixed to the branches near the walnuts using tie-wraps, and the distance from the walnut fruit was within 10 cm. The y-axis was set in the same direction as the growth direction of the tree branch, and the z-axis was set in the perpendicular direction making the angle with the vertical direction smaller. The measurements were transmitted to a computer through a four-channel constant current adapter (CT5204) and a data-acquisition card (E1608) and then output through DAQami software (v4.2.1). The software output curves in acceleration over time in the three directions of the walnuts. Moreover, the motion morphology of the walnuts during vibration harvesting was recorded by two high-speed cameras (Freefly Wave high-speed camera, Freefly Company, Washington, DC, USA), which output images 50 times slower with a resolution of 2048 by 1024 pixels. To record the vibration response of walnuts from different angles, the two high-speed cameras were positioned on two mutually perpendicular planes, and three fill lights (Aputure 1200d, Shenzhen Aputure Company, Shenzhen, China) were used to obtain clearer images. To maintain the focus on the walnuts and ensure the clarity of observation, the branches and leaves near the walnuts in the images taken by the two high-speed cameras were pruned before the experiment.

In each run of the experiment, the triaxial acceleration sensor and high-speed cameras were first turned on to record the experimental data, and the vibration harvesting device was then run for 15 s. If a target walnut did not fall from the tree within 15 s of vibration, the frequency or amplitude was increased to continue the experiment. If the target walnut fell, another walnut that had not fallen from the tree was selected to continue the experiment. The experiment with the same parameters was repeated three times on different trees.

4. Results and Discussion

4.1. Motion Trajectory and Dropping Position of Walnuts in Vibration Harvesting

Figure 4 shows the motion morphology of walnuts at different vibration frequencies and amplitudes, including the motion trajectory and dropping position. Figures 5 and 6 show the detailed motion trajectory and dropping position, respectively. Figure 5 shows the motion of a walnut from one end point to the other and the almost symmetrical return process in one period. Figure 6 shows four motion moments of the dropping process, namely the moments of the fruit moving to the end point, about to drop, dropping, and after dropping. In the figures above (Figures 4–6), a red solid line shows the motion track of the centroid of the walnut in the image under a vibration response, and the dropping position is also marked. In Figures 4 and 5, the motion trajectory of walnuts is the motion track of the walnut centroid drawn by comparing with the motion video recorded by the high-speed camera, and in Figure 5, by intercepting several positions of the walnut in one motion cycle, the motion of walnuts recorded by the high-speed camera is approximately reflected, which intuitively shows that the motion trajectory of the walnuts resembles an ellipse. The dropping position of walnuts is determined by drawing the motion trajectory and observing the fruit's motion position when fracture occurs between the fruit and the fruit handle through the video recorded by the high-speed camera. As in Figure 6, it shows several moments before and after the dropping moment of the walnuts. By determining the position of the walnuts before and after dropping, the dropping moment can be determined, and the position of this moment at both end points of the walnut motion trajectory can be further obtained. The conclusion that the dropping position is at the end points is consistent with the theoretical model that the maximum detachment force appears at the end point, and walnuts are most likely to drop. In general, it is seen that the actual motion trajectory of the walnuts resembles an ellipse, which is consistent with the theoretical modeling. Moreover, the dropping points are at both end points of the motion trajectory, which is consistent with the detachment mechanism in the theoretical derivation.

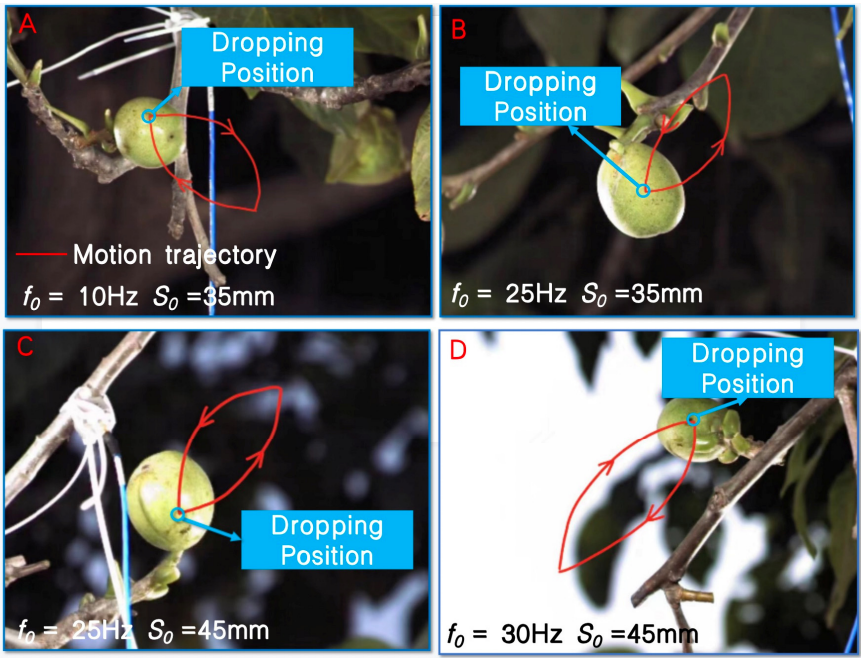


Figure 4. Motion morphology of walnuts at different frequencies f_0 and amplitudes S_0 of vibration: (**A**) f_0 = 10 HZ, S_0 = 35 mm; (**B**) f_0 = 25 HZ, S_0 = 35 mm; (**C**) f_0 = 25 HZ, S_0 = 45 mm; (**D**) f_0 = 30 HZ, S_0 = 45 mm.

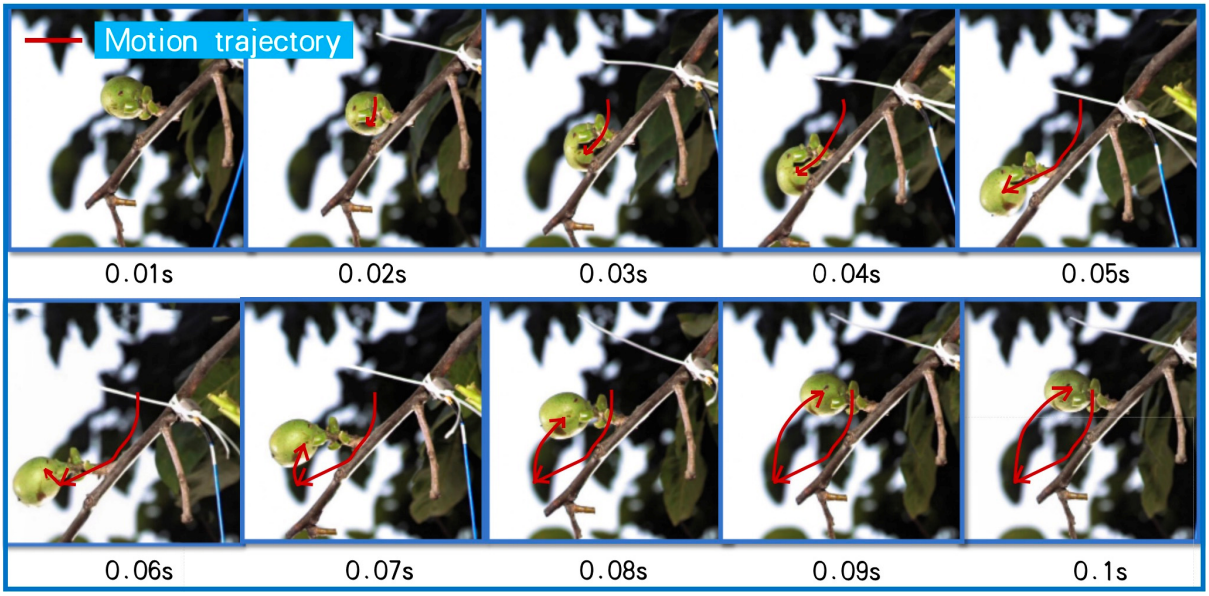


Figure 5. Motion trajectory of the vibration response of walnuts in one period.

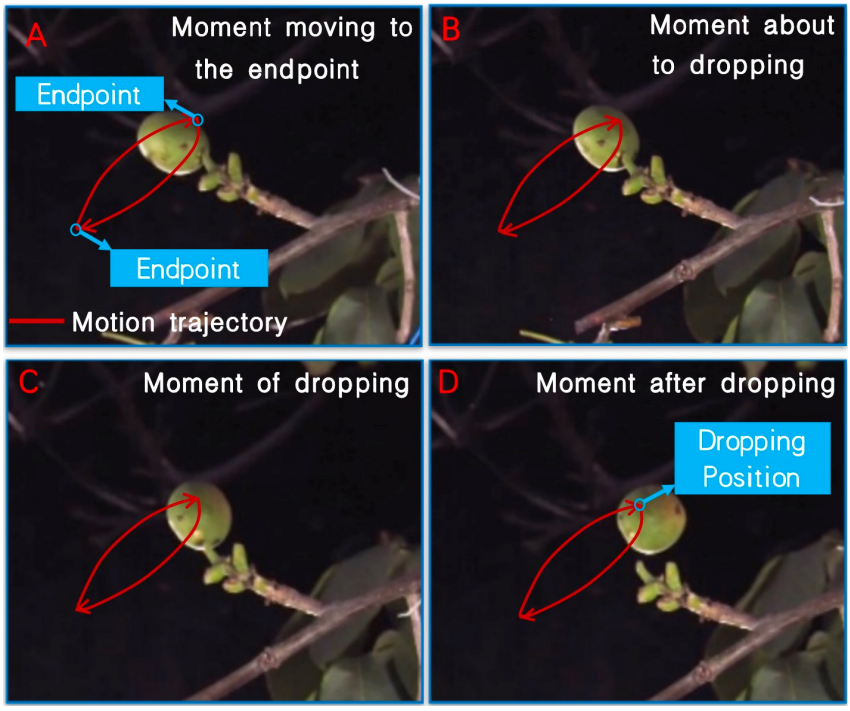


Figure 6. Dropping position of the vibration response of walnuts in one period: (**A**) the walnut's position when moving to the end point; (**B**) the walnut's position when about to drop; (**C**) the walnut's position when dropping; (**D**) the walnut's position when after dropping.

The experimental results of the vibration response trajectory and falling position of the walnuts verifies the theoretical model developed in Section 2. The vibration response of fruits has been presented as the synthesis of multiple motions, such as pendulum, tilting, twisting, and beam-column [16,29]. In the case of jujube fruits, different motions have been observed when the fruits were vibrated on an experimental platform. It was found that twisting rarely occurs in the actual mechanical vibration harvesting process; the motion of jujube fruits was a pendulum when the fruits were vibrated on a horizontal plane, whereas when the fruits were vibrated on a vertical plane, the motion presented as a pendulum

and beam-column motion, and the force was maximum at the end point [13,22]. In this paper, the motion morphology of the walnuts under vibration harvesting was analyzed on the theoretical level, adopting the synthesis and resolution of motion, and the motion was found to mainly present as a combination of horizontal linear motion with varied acceleration and pendulum, as well as vertical linear motion with varied acceleration (i.e., beam-column motion). Additionally, the trajectory of the synthesized motion resembled an ellipse, which is consistent with the feature point trajectory curve of fruits in three-dimensional space seen in a rigid–flexible coupling simulation experiment [30], and the dropping position of walnuts is concentrated at both end points of the motion trajectory, which is because the fracture occurs at the moment of maximum detachment force, and the moment when the detachment force is maximum is when the fruit moves to the end point. However, in contrast with previous studies that only conducted experiments on an experimental platform or computer simulation analysis, a field test was conducted in the present study. The response of walnuts at different frequencies and amplitudes was recorded with high-speed cameras, and the video of the motion morphology of walnuts in the experiment was compared with the theoretical analysis to verify the theoretical model. The motion trajectory and dropping position of walnut fruits under vibration harvesting were thus obtained, and the theoretical model was verified, which included the motion morphology and detachment force.

4.2. Relationship between the Detachment Force and the Vibration Frequency and Amplitude

The field test also investigated the changes in the vibration response frequency and acceleration at the same position near the walnut fruits under forced vibration during vibration harvesting at different vibration frequencies f_0 and amplitude S_0. Because the maximum difference between the fruits' input frequency and response frequency can exceed 53% [19] and the distance from the location of vibration input to the fruit is far greater than the distance from the sensor to the fruit, the experiment in this paper approximately considers that the response of the branches near the fruit is the same as that of the fruit. The acceleration of the walnuts over time measured by the triaxial acceleration sensor is shown in Figure 7. In subsequent analysis, the acceleration at the point of measurement was taken as the vector sum of the maximum acceleration, and the frequency was obtained by analyzing the change in acceleration per unit time.

Figure 8a shows the response frequencies at the position of the fruit f_1 for different vibration frequencies f_0 of the harvesting device. Figure 8b shows the response accelerations at the position of the fruit a_1 for different vibration amplitudes S_0 at the harvesting device. The fitting results show that there is a linear relationship between f_1 and f_0 and between a_1 and S_0. The slopes of the lines sightly differ because different trees were selected in the experiment to obtain universal results, and different trees have different physical properties in field testing [7,8,14], leading to different transmission rates of frequency and amplitude. Additionally, the difference between f_1 and f_0 was approximately 50 percent because the diameter, crotch angle, and connection points of branches affect vibration transmission [8,10]. There is deviation between the data points and the fitting lines. In a group of experimental runs, walnuts at different positions of the same tree were selected as the experimental object when the walnut at the observation position fell off, and the attenuation rate of the vibration frequency and amplitude transmitted to different positions differed because of the diversity of the structures of the trees [16–18]. In general, the response frequency f_1 and response acceleration a_1 near the fruits are proportional to the vibration frequency f_0 and the input amplitude S_0, respectively. The response amplitude S_1 is the double integral of the response acceleration a_1 to time t, and S_1 is thus proportional to a_1 during the same period. Therefore, the response amplitude S_1 is proportional to the vibration amplitude S_0. S_1 and f_1 are then expressed as $S_1 = \beta_1 S_0$ and $f_1 = \beta_2 f_0$. β_1 and β_2 are, respectively, the decay rates of S_0 and f_0. Therefore, Equation (13) is rewritten as

$$F_E = \left(\vec{\varepsilon_1} + \vec{\varepsilon_2} + \vec{\varepsilon_3}\right)\beta_1\beta_2 S_0 f_0^2. \tag{19}$$

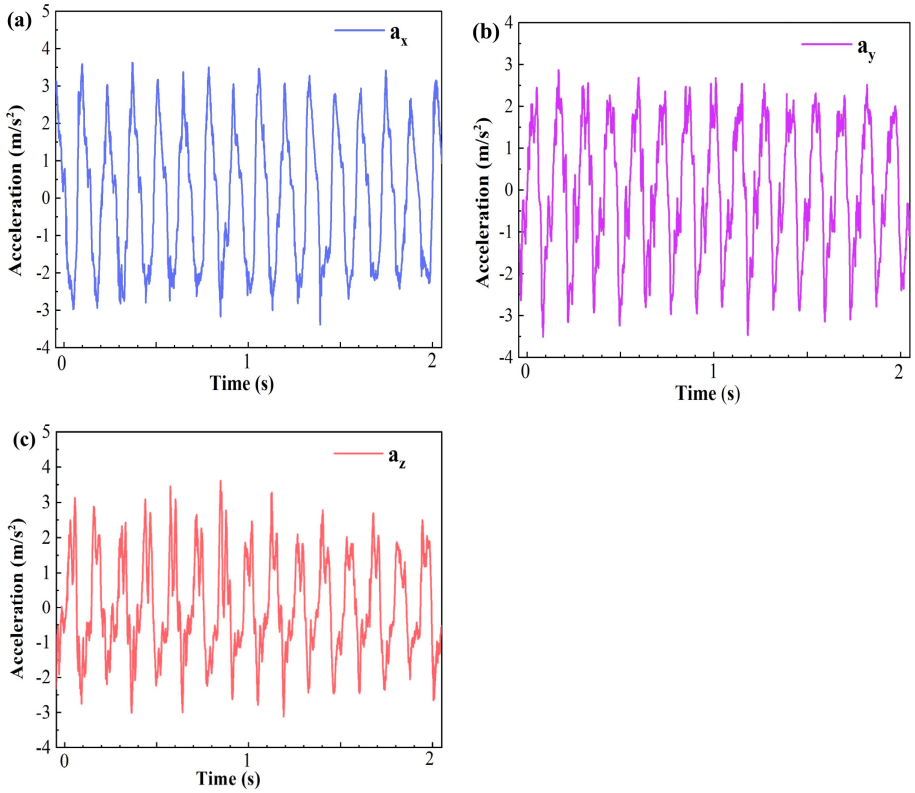


Figure 7. Acceleration of the walnuts versus time at: (**a**) *x*-axis; (**b**) *y*-axis; (**c**) *z*-axis measured by the triaxial acceleration sensor.

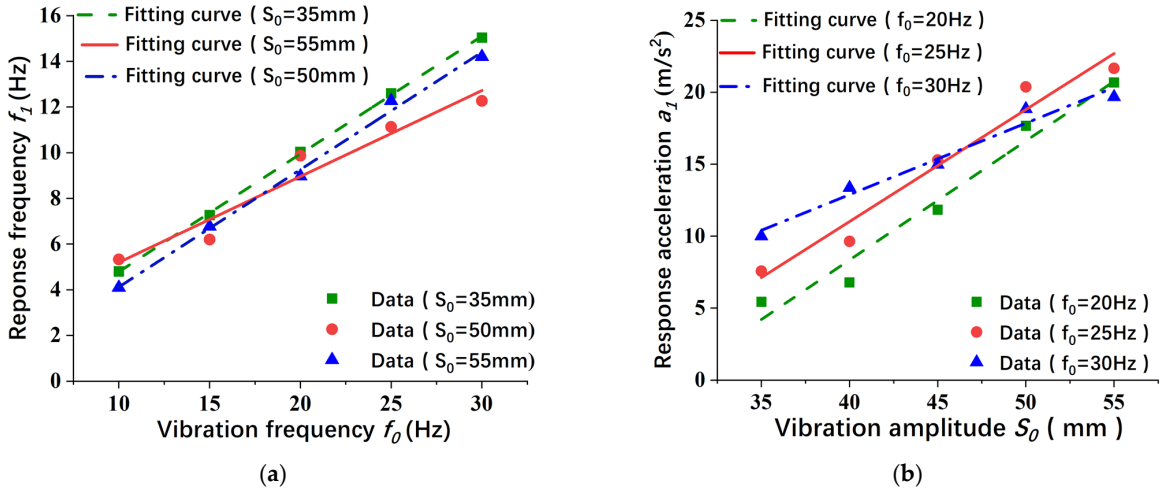


Figure 8. (**a**) Response frequency of the walnut f_1 for different vibration frequencies of the device f_0 and different vibration amplitudes S_0 (where symbols represent experimental data and lines represent the fitting curves); (**b**) response accelerations of the walnut a_1 for different vibration amplitudes of the device f_0 and different vibration amplitudes S_0 (where symbols represent data and lines represent the fitting curves).

This equation expresses the relationship between the detachment force and vibration frequency and amplitude. Furthermore, the relationship between the vibration response and vibration frequency and amplitude is intuitively understood in that the magnitude of the detachment force reflects the vibration response. This result indicates that in order to achieve a better vibration response and improve the fruit harvesting rate, vibration frequency and vibration amplitude should be considered comprehensively.

The main factors affecting the vibration response of walnuts under vibration harvesting are the vibration frequency, amplitude, position, and duration [20,30]. For a single harvest of the same tree, the point of vibration is fixed. The vibration duration affecting the harvest rate of walnuts relates to the effect of fatigue stress under low-frequency vibration [22] and has no effect on the vibration response of fruits under a single vibration. Accordingly, this paper focused on the vibration frequency and amplitude, which are the main factors of the vibration response of walnuts under vibration in a single operation within a fixed time. As the vibration frequency and amplitude increase, the detachment force strengthens, enhancing the vibration response at the walnut fruits and increasing the harvesting efficiency [19,24,25]. By conducting model simulations and summarizing the results of experiments, the cited studies found a general relationship between the vibration response of walnuts and the vibration frequency and amplitude in the harvesting process. In the present study, the detachment mechanism of the walnut vibration response under vibration harvesting was analyzed at the theoretical level and verified by experiments. Moreover, an equation of the relationship between the detachment force and the vibration frequency and amplitude was established in this paper. The equation shows that the detachment force of walnut fruits under forced vibration is proportional to $S_1{F_1}^2$. In contrast with only determining the relationship between the vibration response of fruits and a certain vibration parameter, in this study, the relationship was expanded to the joint action of the vibration frequency and amplitude, with the association being established using a specific equation in a more intuitive way. The relationship provides a theoretical explanation for the experimental light shaking at low frequency and high amplitude generating a low response acceleration and high damage level compared with the use of a trunk shaker [31] and suggests that the vibration frequency and amplitude need to be appropriately and effectively combined for vibration harvesting [24,26]. Additionally, the equation provides a reference for the design of the vibration harvesting device, and its use is expected to increase the harvesting rate of walnuts under vibration harvesting and avoid improper parameter design in the mere pursuit of resonance harvesting, which reduces the service life of a harvesting machine and damages trees [19,27]. The importance of the present study is that it presents the vibration response of walnuts during actual and non-resonant vibration harvesting.

5. Conclusions

The specific vibration response of walnuts is important to walnut vibration harvesting owing to its close relation to the dropping of the fruit. To explore the vibration response, including the motion morphology (motion trajectory and dropping position) and detachment force, this study established a theoretical model of walnuts during vibration harvesting through the synthesis and decomposition of motion and forces. Additionally, a field test was designed and carried out to verify the theoretical model. The main conclusions are summarized as follows.

1. Theoretical and experimental results both showed that the motion trajectory of the walnuts during vibration harvesting is similar to an ellipse, and the dropping positions are at the two end points of the trajectory.
2. For vibration harvesting of walnuts under actual harvesting conditions, the response amplitude of the walnuts is proportional to the vibration amplitude of the device. Additionally, the response frequency of the walnuts is proportional to the vibration frequency of the device, with the attenuation rate being approximately 50%.
3. Using the theoretical model and extending the experiment, the equation for the relationship between the detachment force and the vibration response and amplitude was obtained, which shows the detachment force is proportional to the vibration amplitude and the square of the vibration frequency. This relationship further reflects that in order to achieve better vibration response and improve the fruit harvesting rate, vibration frequency and vibration amplitude should be considered comprehensively.

Author Contributions: Data curation, J.C.; Writing—original draft, C.L.; Supervision, D.X. All authors have read and agreed to the published version of the manuscript.

Funding: This research was funded by National Key Research and Development Program of China grant number 2019YFD1002401.

Data Availability Statement: Not applicable.

Conflicts of Interest: The funders had no role in the design of the study; in the collection, analyses, or interpretation of data; in the writing of the manuscript; or in the decision to publish the results.

Abbreviations

Notation	
m	Weight of walnut fruits (kg)
θ_0	Angle of F_0 with respect to the horizontal direction (deg)
θ_H	Maximum angle of the horizontal pendulum (deg)
F_0	Vibration force at the input end (N)
F_1	Excitation force at the fruits (N)
F_{1v}	Component of F_1 in the vertical direction (N)
F_{1H}	Component of F_1 in the horizontal direction (N)
F_E	Maximum resultant external force of synthesized motion (N)
F_{HE}	Resultant external force in the horizontal direction (N)
F_{vE}	Resultant external force in the vertical direction (N)
F_{BE}	Resultant external force at point B (N)
F_{DE}	Resultant external force at point D (N)
F_n	Centripetal force of the horizontal pendulum (N)
F_{DEP}	Resultant external force of the pendulum at point D (N)
F_{DEL}	Resultant external force of linear motion with varying acceleration at point D (N)
ε_1	Vector in the same direction as F_{BE}
ε_2	Vector in the same direction as F_{DEL}
ε_3	Vector in the same direction as F_{DEP}
γ_1	Ratio of S^*_{1H} to S_{1H}
S_0	Vibration amplitude (mm)
S_1	Response amplitude at the fruits (mm)
S_{1v}	Component of S_1 in the vertical direction (mm)
S_{1H}	Component of S_1 in the horizontal direction (mm)
S^*_{1H}	Displacement of the horizontal pendulum (mm)
β_1	Decay rate of F_0
β_2	Decay rate of S_0
β_3	Decay rate of f_0
β_4	Ratio of F_n to F_{1H}
f_0	Vibration frequency (Hz)
f_1	Vibration response frequency of fruits (Hz)
$v_{B'}$	Velocity at point B′ (m/s)
$v_{D'P}$	Velocity of horizontal pendulum at D′ point (m/s)
$v_{D'Px}$	Component of $v_{D'P}$ in horizontal direction (m/s)
$v_{D'Py}$	Component of $v_{D'P}$ in the vertical direction (m/s)
$v_{D'L}$	Velocity of horizontal linear motion with varying acceleration at point D′ (m/s)
t_{BO}	Time at which $v_{B'}$ decreases to zero
t_{DO}	Time at which $v_{D'L}$ or $v_{D'P}$ decreases to zero
α_1	Ratio of t_{BO} in the half motion cycle
α_2	Ratio of t_{DO} in the half motion cycle

References

1. Thomson, G.; McCaskill, M.; Goodwin, I.; Kearney, G.; Lolicato, S. Potential impacts of rising global temperatures on Australia's pome fruit industry and adaptation strategies. *N. Zeal. J. Crop Hort.* **2014**, *42*, 21–30. [CrossRef]
2. Webb, B.K.; Hood, C.E.; Jenkins, W.H.; Veal, C.D. Development of an over-the-row peach harvester. *Trans. ASAE* **1973**, *16*, 450–455. [CrossRef]
3. Churchill, D.B.; Sumner, H.R. A new system for raking and picking up oranges. *Trans. ASAE* **1977**, *20*, 617–620. [CrossRef]

4. Churchill, D.B.; Hedden, S.L. A double-sided rake-pickup machine for citrus. *Trans. ASAE* **1983**, *26*, 1034–1036. [CrossRef]
5. Sanders, K.F. Orange harvesting systems review. *Biosyst. Eng.* **2005**, *90*, 115–125. [CrossRef]
6. Hedden, S.L.; Churchill, D.B.; Whitney, J.D. Trunk shakers for citrus harvesting—Part II: Tree growth, fruit yield and removal. *Appl. Eng. Agric.* **1988**, *4*, 102–106. [CrossRef]
7. Du, X.; Chen, D.; Zhang, Q.; Scharf, P.A.; Whiting, M.D. Dynamic responses of sweet cherry trees under vibratory excitations. *Biosyst. Eng.* **2012**, *111*, 305–314. [CrossRef]
8. Erdoğan, D.; Güner, M.; Dursun, E.; Gezer, İ. Mechanical harvesting of apricots. *Biosyst. Eng.* **2003**, *85*, 19–28. [CrossRef]
9. Zhang, W.; Yao, W.; Xv, X. Study of picking method for carya cathayensis. *Appl. Mech. Mater.* **2011**, *1366*, 71–78.
10. Du, X.; Wu, C.; He, L.; Tong, J. Dynamic characteristics of dwarf Chinese hickory trees under impact excitations for mechanical fruit harvesting. *Int. J. Agric. Biol. Eng.* **2015**, *8*, 17–25.
11. Bentaher, H.; Haddar, M.; Fakhfakh, T.; Mâalej, A. Finite elements modeling of olive tree mechanical harvesting using different shakers. *Trees* **2013**, *27*, 1537–1545. [CrossRef]
12. Tinoco, H.A.; Ocampo, D.A.; Peña, F.M.; Sanz-Uribe, J.R. Finite element modal analysis of the fruit-peduncle of *Coffea arabica* L. var. Colombia estimating its geometrical and mechanical properties. *Comput. Electron. Agric.* **2014**, *108*, 17–27. [CrossRef]
13. Zhou, J.; Xu, L.; Zhang, A.; Hang, X. Finite element explicit dynamics simulation of motion and shedding of jujube fruits under forced vibration. *Comput. Electron. Agric.* **2022**, *198*, 107009. [CrossRef]
14. Castro-García, S.; Blanco-Roldán, G.L.; Gil-Ribes, J.A.; Agüera-Vega, J. Dynamic analysis of olive trees in intensive orchards under forced vibration. *Trees* **2008**, *22*, 795–802. [CrossRef]
15. Zhou, J.; He, L.; Zhang, Q.; Karkee, M. Effect of excitation position of a handheld shaker on fruit removal efficiency and damage in mechanical harvesting of sweet cherry. *Biosyst. Eng.* **2014**, *125*, 36–44. [CrossRef]
16. He, L.; Liu, X.; Du, X.; Wu, C. In-situ identification of shaking frequency for adaptive vibratory fruit harvesting. *Comput. Electron. Agric.* **2020**, *170*, 105245. [CrossRef]
17. Zhou, J.; Xu, L.; Liu, G.; Xuan, Y.; Zhou, H.; Jiang, H. Frequency response curves and dynamic characteristics of a ginkgo tree in different growth periods. *Trans. ASABE* **2020**, *63*, 1673–1684. [CrossRef]
18. He, L.; Zhou, J.; Du, X.; Chen, D.; Zhang, Q.; Karkee, M. Energy efficacy analysis of a mechanical shaker in sweet cherry harvesting. *Biosyst. Eng.* **2013**, *116*, 309–315. [CrossRef]
19. Leone, A.; Romaniello, R.; Tamborrino, A.; Catalano, P.; Peri, G. Identification of vibration frequency, acceleration, and duration for efficient olive harvesting Using a Trunk Shaker. *Trans. ASABE* **2015**, *58*, 19–26.
20. Castro-García, S.; Blanco-Roldán, G.L.; Gil-Ribes, J.A. Frequency response of Pinus Pinea, L. for selective cone harvesting by vibration. *Trees* **2011**, *25*, 801–808. [CrossRef]
21. Castro-Garcia, S.; Sola-Guirado, R.R.; Gil-Ribes, J.A. Vibration analysis of the fruit detachment process in late-season 'Valencia' orange with canopy shaker technology. *Biosyst. Eng.* **2018**, *170*, 130–137. [CrossRef]
22. Zhou, J.; Xu, L.; Xuan, Y.; Xu, Y.; Liu, G. Shedding frequency and motion of jujube fruits in various excitation modes. *Trans. ASABE* **2020**, *63*, 881–889. [CrossRef]
23. He, L.; Zhang, X.; Ye, Y.; Karkee, M.; Zhang, Q. Effect of shaking location and duration on mechanical harvesting of fresh market apples. *Appl. Eng. Agric.* **2019**, *35*, 175–183. [CrossRef]
24. Coelho, A.L.F.; Santos, F.L.; Pinto, F.A.C.; Queiroz, D.M. Detachment efficiency of fruits from coffee plants subjected to mechanical vibrations. *Pesq. Agrop. Trop.* **2015**, *45*, 406–412. [CrossRef]
25. Savary, S.K.J.U.; Ehsani, R.; Schueller, J.K.; Rajaraman, B.P. Simulation study of citrus tree canopy motion during harvesting using a canopy shaker. *Trans. ASABE* **2010**, *53*, 1373–1381. [CrossRef]
26. Tsatsarelis, C.A. Vibratory olive harvesting: The response of the fruit-stem system to fruit removing actions. *J. Agric. Eng. Res.* **1987**, *38*, 77–90. [CrossRef]
27. Castro-Garcia, S.; Blanco-Roldán, G.L.; Ferguson, L.; González-Sánchez, E.J.; Gil-Ribes, J.A. Frequency response of late-season 'Valencia' orange to selective harvesting by vibration for juice industry. *Biosyst. Eng.* **2017**, *155*, 77–83. [CrossRef]
28. Tombesi, S.; Poni, S.; Palliotti, A.; Farinelli, D. Mechanical vibration transmission and harvesting effectiveness is affected by the presence of branch suckers in olive trees. *Biosyst. Eng.* **2017**, *158*, 1–9. [CrossRef]
29. Zhou, J.; He, L.; Karkee, M.; Zhang, Q. Analysis of shaking-induced cherry fruit motion and damage. *Biosyst. Eng.* **2016**, *144*, 105–114. [CrossRef]
30. Wei, J.; Yang, G.; Yan, H.; Jing, B.; Yu, Y. Rigid-flexible coupling simulation and experimental vibration analysis of pistachio tree for optimal mechanized harvesting efficiency. *Mech. Adv. Mater. Struct.* **2021**, *28*, 2360–2369. [CrossRef]
31. Ortiz, C.; Torregrosa, A.; Castro-García, S. Citrus fruit movement assessment related to fruit damage during harvesting with an experimental low-frequency–high-amplitude device. *Agronomy* **2022**, *12*, 1337. [CrossRef]

Disclaimer/Publisher's Note: The statements, opinions and data contained in all publications are solely those of the individual author(s) and contributor(s) and not of MDPI and/or the editor(s). MDPI and/or the editor(s) disclaim responsibility for any injury to people or property resulting from any ideas, methods, instructions or products referred to in the content.